Case Studies in Thermal Engineering 5 (2015) 134–142

Contents lists available at ScienceDirect

Case Studies in Thermal Engineering

journal homepage: www.elsevier.com/locate/csite

A numerical study on helical vortices induced by a short twisted tape in a circular pipe

Wen Liu, Bofeng Bai*

State Key Laboratory of Multiphase Flow in Power Engineering, Xi'an Jiaotong University, Xi'an 710049, PR China

ARTICLE INFO

Article history:
Received 24 December 2014
Received in revised form
4 March 2015
Accepted 12 March 2015
Available online 14 March 2015

Keywords:
Helical vortices
Swirling flow
Twisted tape
Vorticity

ABSTRACT

Helical vortices, as one kind of secondary flows, are recently observed downstream of the short twisted tape. The behaviors of vortices, which have significant effects on the efficiency of twisted tape, are not well understood. As such, the formation and development of helical vortices induced by the short twisted tape are studied numerically. The results show that two symmetrical stable helical vortices are present downstream of the twisted tape. The values of radial velocities cannot be neglected due to the presence of the vortices. The vortices form in the twisted tape and remain the structure downstream of the twisted tape. Torsion promotes the formation of helical vortices. The intensities of helical vortices decay along the streamwise direction. With the increasing Reynolds numbers, the intensities of helical vortices increase, and the trend is in agreement with the swirl intensities. The intensities of helical vortices decay slowly compared with the intensities of swirling flow.

© 2015 The Authors. Published by Elsevier Ltd. This is an open access article under the CC BY-NC-ND license (http://creativecommons.org/licenses/by-nc-nd/4.0/).

1. Introduction

Full length twisted tape insert has been widely applied in industry, as a simple and cheap continuous swirl flow device for heat transfer augmentation in heat exchangers. The penalty of the present technique is the increase of friction pressure drop. Several modifications of twisted tape have been reported in literatures, such as short inlet tapes, serrated tapes and intermittently spaced tapes. The primary motive in these variations is to reduce the pressure drop while maintaining the thermal performance of a full length insert.

Full length twisted tape has been investigated for a long time, researches [1–3] mainly focused on heat transfer and friction coefficient, only a few studies regarding the vortex structure. Double helical longitudinal vortices are observed in the turbulent flow field through measurement [4]. The vortex structure in the laminar flow is the same, confirmed through smoke flow visualizations [5] and computational simulations [6]. However, the visualizations and simulations about vortex motion are restricted to the secondary flow in fully developed flow. The formation and development of vortices, which have significant effects on the vortex motion in the fully developed flow induced by full length twisted tape, are not well understood. This limits the enhancement of heat transfer.

Short twisted tape is a more promising embodiment [7]. The tape is long enough to initiate swirl, and decays in the subsequent empty pipe section. The decay region without the twisted tape seriously reduces the pressure drop, while the improvement of enhancing heat transfer is maintained [8,9]. One significant existing problem of the technique is the limited

* Corresponding author.
E-mail address: bfbai@mail.xjtu.edu.cn (B. Bai).

http://dx.doi.org/10.1016/j.csite.2015.03.003
2214-157X/© 2015 The Authors. Published by Elsevier Ltd. This is an open access article under the CC BY-NC-ND license (http://creativecommons.org/licenses/by-nc-nd/4.0/).

Nomenclature

A	pipe cross section area, m^2
D	pipe diameter, m
D_H	hydraulic diameter, m
H	180° twist pitch, m
I	turbulence intensity
J^n_{ABS}	absolute vorticity flux, s^{-1}
k	turbulent kinetic energy, $m^2\ s^{-2}$
R	pipe radius, m
r	distance in radial direction, m
Re	Reynolds number
S	swirl number, $=\left(\int \rho u_a u_t r dA\right)/\left(R\int \rho u_a^2 dA\right)$[18]
U_b	inlet velocity, $m\ s^{-1}$
u	fluid velocity, $m\ s^{-1}$
u_a	axial fluid velocity, $m\ s^{-1}$
u_i	mean fluid velocity, $m\ s^{-1}$
u_r	radial fluid velocity, $m\ s^{-1}$
u_t	tangential fluid velocity, $m\ s^{-1}$
u'	fluctuating fluid velocity, $m\ s^{-1}$
$\overline{u'_i}$	mean fluctuating fluid velocity, $m\ s^{-1}$
z	distance in Z direction, m

Greek letters

α	inverse effective Prandtl numbers
δ	tape thickness, m
δ_{ij}	Kroneker delta
ε	turbulent kinetic energy dissipation rate, $m^2\ s^{-3}$
θ	angle, °
μ_t, μ_{eff}	turbulent viscosity, Pa s
ρ	density, $kg\ m^{-3}$
ω_a	axial vorticity component, s^{-1}
ω_{da}	dimensionless of axial vorticity component

Subscripts

a	in axial direction
r	in radial direction
t	in tangential direction

awareness concerning vortex behavior in the swirl flow which suppresses its application and structure optimization. Recently, the secondary motion in the swirling flow downstream of a 180° twisted tape was studied, two corotating helical vortices were observed in the experiment [10,11]. However the helical vortices motion, such as vortex formation and development, are not well understood. The most dominant heat transfer enhancement mechanism of circular tube fitted with twisted tape is the vortices motion generated by the tape. Grasping the underlying mechanism of vortices motions is essential to enhance heat transfer, and meanwhile reduce energy consumption.

The turbulent swirling flow is studied numerically in this study, to clarify the helical vortices hydro-dynamics in the swirling flow induced by the short twisted tape. Helical vortices formation and development are reported. The present study improves the understanding of the vortices formation and development in the swirling flow, thus enabling the development of more efficient heat exchanger devices.

2. Numerical simulation

2.1. Geometry model and mesh generation

The 180 degree twisted tape considered is a typical short twisted tape. Fig. 1 shows the circular pipe, twisted tape geometry and notations. In order to correlate the calculation with the experimental data [11], the structure parameters of the simulation are the same with the parameters in the experiment. The pipe diameter (D) is 25.40 mm, the pipe length (L)

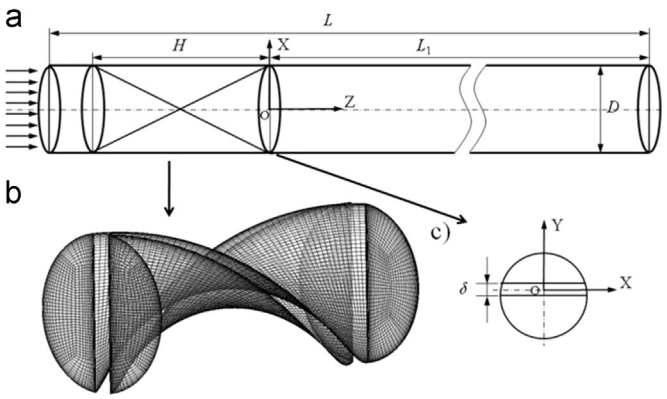

Fig. 1. Geometry model of a circular pipe with a twisted tape: (a) computational domain, (b) twisted tape showing the structure grids and (c) cross section at $z=0$, the direction of arrows represents the flow direction.

is 18.50D, the length of test section (L_1) 15.75D, the pitch (H) 2.36D, the tape thickness (δ) 0.12D. Cartesian coordinate system is used, the origin point of coordinate is located at the center of the twisted tape tailing edge. The direction of gravity is along the negative X axis.

The geometry of the modeled pipe system is divided by structured hexahedron grids. In the mesh independence test (507,520, 719,654 and 1,067,879 cells are tested), results show that 719,654 cells already satisfy mesh independent. The region adjacent to the wall was refined using a denser mesh to numerically replicate the rapid change of the velocity gradient across the boundary layer for the pipe wall and twisted tape surface. The mesh of twisted tape section is shown in Fig. 1.

2.2. Description of numerical model

For a steady, incompressible and iso-thermal turbulent flow, the Reynolds averaged continuity and momentum equations, are given in the tensor form as:

$$\frac{\partial u_i}{\partial x_i} = 0 \tag{1}$$

$$\rho\frac{\partial(u_i u_j)}{\partial x_j} = -\frac{\partial p}{\partial x_i} + \frac{\partial}{\partial x_j}\left[\mu\left(\frac{\partial u_i}{\partial x_j} - \rho\overline{u'_i u'_j}\right)\right] \tag{2}$$

where ρ is fluid density, u_i a mean component of velocity, p the pressure, μ the dynamic viscosity, and u' a fluctuating component of velocity. Repeated i, j indices indicate summation from one to three. $-\rho\overline{u'_i u'_j}$ is known as the Reynolds stresses which can be modeled by directly solving the Reynolds stress equations and by exploiting the Boussinesq hypothesis. The former is called Reynolds stress model (RSM), and for the latter, the effect of turbulent eddy motions is described and incorporated into the turbulent viscosity term (μ_t).

As the present study considers swirling flow in the pipe, the Renormalization group (RNG) k-ε turbulence model and RSM were used widely to describe swirling flows [12,13]. In the present work, 3D (three dimension) swirling flow is induced by the twisted tape, its streamlines curve sharply. Both RNG k-ε turbulence model and RSM are used, in order to determine a turbulence model in better agreement with experimental results.

2.2.1. RNG k-ε turbulence model

The RNG k-ε model is an example of two-equation models that use Boussinesq hypothesis to model Reynolds stresses. In the RNG k-ε model transport equations for the turbulence kinetic energy and turbulence dissipation are solved:

$$\frac{\partial}{\partial x_i}(\rho k u_i) = \frac{\partial}{\partial x_j}\left(\alpha_k \mu_{eff}\frac{\partial k}{\partial x_j}\right) + G_k - \rho\varepsilon + S_k \tag{3}$$

$$\frac{\partial}{\partial x_i}(\rho \varepsilon u_i) = \frac{\partial}{\partial x_j}\left(\alpha_\varepsilon \mu_{eff}\frac{\partial \varepsilon}{\partial x_i}\right) + C_{1\varepsilon}\frac{\varepsilon}{k}G_k - C_{2\varepsilon}\rho\frac{\varepsilon^2}{k} - R_\varepsilon + S_\varepsilon \tag{4}$$

where G_k represents the production of turbulence kinetic energy. The quantities α_k and α_ε are the inverse effective Prandtl numbers for k and ε, respectively. $C_{1\varepsilon}$ and $C_{2\varepsilon}$ are model constants, equal 1.42 and 1.68, respectively. μ_{eff} is the effective viscosity. Parameters in Eq. (4) are given by:

$$\left.\begin{aligned}
&\mu_{eff} = \mu_t = \rho C_\mu \frac{k^2}{\varepsilon},\ S = \left(2S_{i,j}S_{i,j}\right)\\
&G_k = -\rho\overline{u'_i u'_i}\frac{\partial u_j}{\partial x_i} = \mu_t S^2\\
&R_\varepsilon = \frac{C_\mu \rho \eta^3\left(1-\eta/\eta_0\right)}{1+\beta\eta^3}\frac{\varepsilon^2}{k},\ \eta = Sk/\varepsilon\\
&S_{i,j} = \frac{1}{2}\left(\frac{\partial u_i}{\partial x_j} + \frac{\partial u_j}{\partial x_i}\right),\ \beta = 0.012,\ \eta_0 = 4.38
\end{aligned}\right\} \tag{5}$$

2.2.2. Reynolds stress model

The RSM includes the effect of anisotropy of turbulence, which yields it superior to models based on Boussinesq approach when simulating highly swirled flows and stress driven secondary flows. The RSM provides one equation for each of the Reynolds stresses as well as one equation for the dissipation of turbulent energy. The transport equations are shown below:

$$\frac{\partial}{\partial x_k}\left(\rho u_k u'_i \bar{u}'_j\right) = \frac{\partial}{\partial x_k}\left[\frac{\mu_t}{\sigma_k}\frac{\partial u'_i \bar{u}'_j}{\partial x_k}\right] + \frac{\partial}{\partial x_k}\left[\mu\frac{\partial}{\partial x_k}\left(u'_i \bar{u}'_j\right)\right] + p\left(\frac{\partial \bar{u}'_i}{\partial x_j} + \frac{\partial u'_j}{\partial x_i}\right) - \rho\left(u'_i \bar{u}'_k \frac{\partial u_j}{\partial x_k} + u'_j \bar{u}'_k \frac{\partial u_i}{\partial x_k}\right) - \frac{2}{3}\delta_{ij}\rho\varepsilon + S_{user} \quad (6)$$

where S_{user} is user-defined source terms. The term on the left hand side of Eq. (6) represents the convection, the terms on the right-hand side represent the turbulent diffusion as proposed by Lien and Leschziner [14], molecular diffusion, stress production, pressure strain, and the dissipation, respectively. The detailed description of those turbulence models can be found in literatures, such as Pope [15], and Fluent User's Guide [16]. The commercial Fluent CFD (computational fluid dynamics) software is used to construct and solve the flow models here.

Those turbulence models are primarily valid for turbulent core flows. The standard wall function has been most widely used, and is chosen here to treat the near wall region.

2.3. Boundary conditions and solver parameters

The working fluid in the model is water at room temperature. At the inlet, a velocity inlet boundary condition is used, the inlet velocity (U_b) is 3.03 m s^{-1}. The turbulence intensity is calculated by $I=0.16(Re_D)^{-1/8}$, where Re_D is the Reynolds number based on the pipe diameter, D. The turbulence intensity is determined to be approximately 4%. The outlet boundary condition is set to an outflow condition. No slip boundary conditions are applied on solid surfaces.

The steady state flow is solved using the software FLUENT. The solver is 3D, pressured based and coupled. The pressure and velocity coupling is handled by using the SIMPLE (Semi-Implicit Method for Pressure Linked Equations) algorithm. The second order upwind schemes are used for momentum, turbulence kinetic energy, turbulence dissipation rate, and Reynolds stresses. The convergence criterion used for the simulation is that the residual of the equations drops more than five orders of magnitude.

2.4. Model validation

The results of tangential and axial velocities compared with the measured data [11] are shown in Fig. 2, to assess the predictive capability of the chosen turbulence models for simulating the strongly swirling flow. Fig. 2 shows the tangential and axial velocities at $z=185$ mm and 150 mm, respectively. The computational results by the RSM show an excellent agreement with the measurement compared with the results calculated by RNG k-ε turbulence model. The RSM should be selected and used for prediction of this kind of flow induced by short twisted tape.

3. Results and discussion

3.1. Vortices structure

The structure of vortices is characterized by ω_{da}, the dimensionless vorticities of axial component. It is defined as follow:

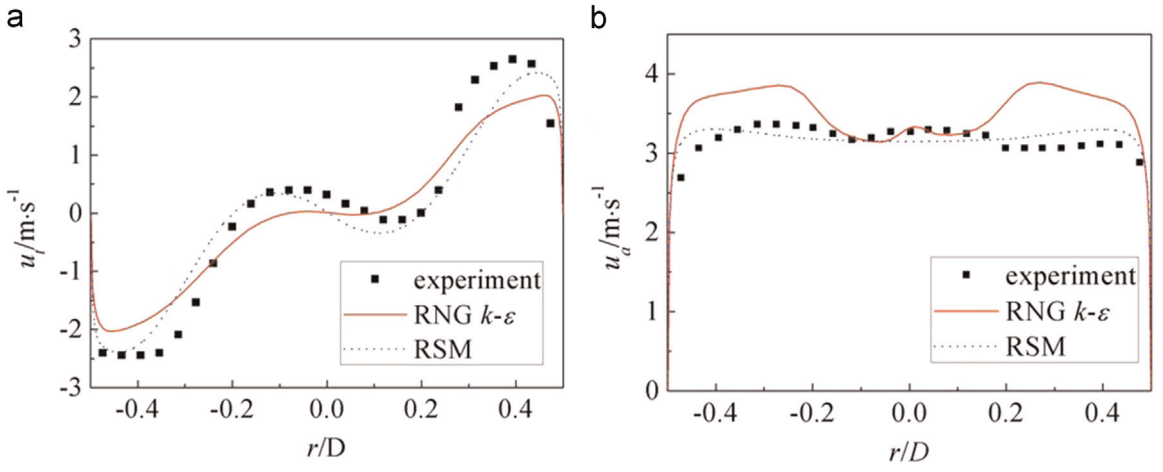

Fig. 2. Comparison of experimental results with tangential and axial velocity on the diameter along Y axis: (a) tangential velocity at $z=185$ mm and (b) axial velocity at $z=150$ mm.

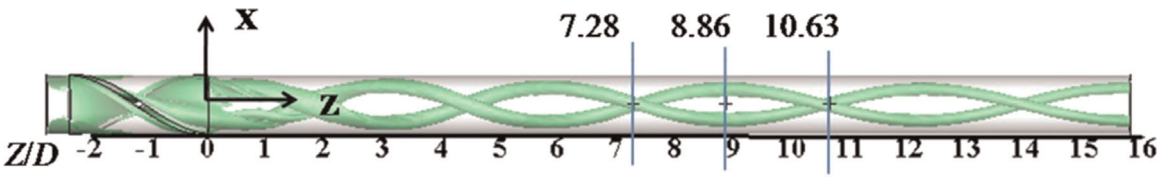

Fig. 3. 3D dimensionless vorticities of axial component ω_{da}, the data values on the iso-surface equal 3.35.

$$\omega_{da} = \frac{\omega_a D}{2U_b} \tag{7}$$

where D is the pipe diameter, ω_a is vorticities of axial component, and U_b is the inlet velocity.

The dimensionless vorticities of axial component (ω_{da}) field in the whole pipe are showed in Fig. 3. The data values on the iso-surface in the figure equal 3.35. As vorticities can reflect the structure of vortices, the distributions of vorticities in Fig. 3 obviously show that the secondary structure induced by the twisted tape is two symmetrical helical vortices. The vortices rotate around the pipe center. In terms of vorticity distribution, two regions of vortices formation and development can be divided. In the twisted tape region, helical vortices form. Out of the twisted tape, helical vortices are developed. In the twisted tape region, vorticities mainly concentrate on the twisted tape surface as fluid twists sharply here. Near the twisted tape outlet, the flow structures of helical vortices are not stable. Away from the twisted tape, the flow structure of vortices gradually become stable. It shows that helical vortices induced by twisted tape are stable, which is important for the investigation of helical vortices dynamics in pipes, as helical vortices in pipes are unstable and easy to breakdown.

The velocity field induced by helical vortices in the pipe is shown in Fig. 4. Tangential velocities at different streamwise positions (z/D=7.28, 8.86 and 10.63) are shown in Fig. 4(a). The tangential velocity increases sharply near the pipe wall, while decreases greatly in the vicinity of the pipe center, which is in good agreement with the experimental results [11]. The tangential velocity gradient increases sharply near the pipe wall, which is benefit for heat transfer enhancement. Radial velocities at different streamwise positions (z/D=7.28, 8.86 and 10.63) and 3D distribution along streamwise are shown in Fig. 4(b) and (c), respectively. As the presence of helical vortices, radial motions are complicated. Two high and two low radial velocity regions present, and those regions are symmetric, shown in Fig. 4(b). The radial velocities directions in these two regions are opposite. Fig. 4(c) shows the data values on the iso-surfaces of dimensionless radial velocity (u_r/U_b) are 0.25 and −0.25, respectively. The structures of those iso-surfaces are two symmetrical helical tubes. The values of radial velocities should not be ignored, compared with the value of fluid inlet velocity U_b. Radial velocities induced by helical vortices promote the fluid mixing.

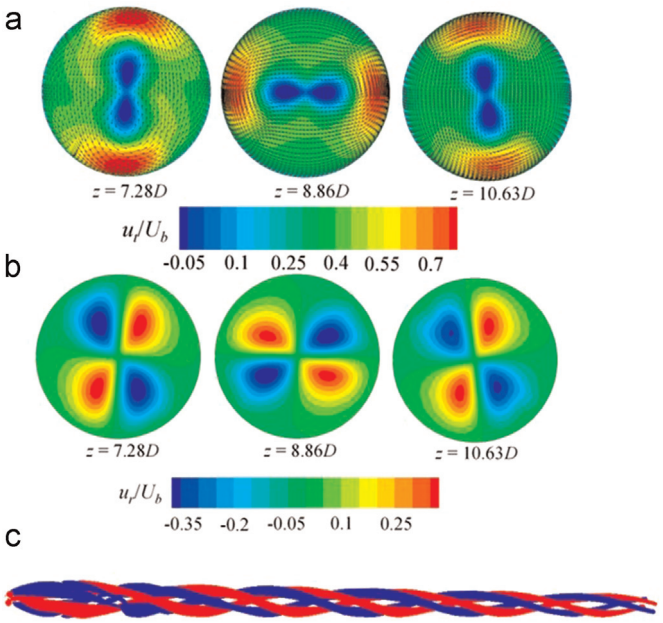

Fig. 4. Dimensionless velocity at different streamwise positions: (a) dimensionless tangential velocity (u_t/U_b) and velocity vector, (b) dimensionless radial velocity (u_r/U_b) and (c) 3D dimensionless radial velocities (u_r/U_b), the data values on the blue and red iso-surface are 0.25 and −0.25, respectively. (For interpretation of the references to color in this figure legend, the reader is referred to the web version of this article.).

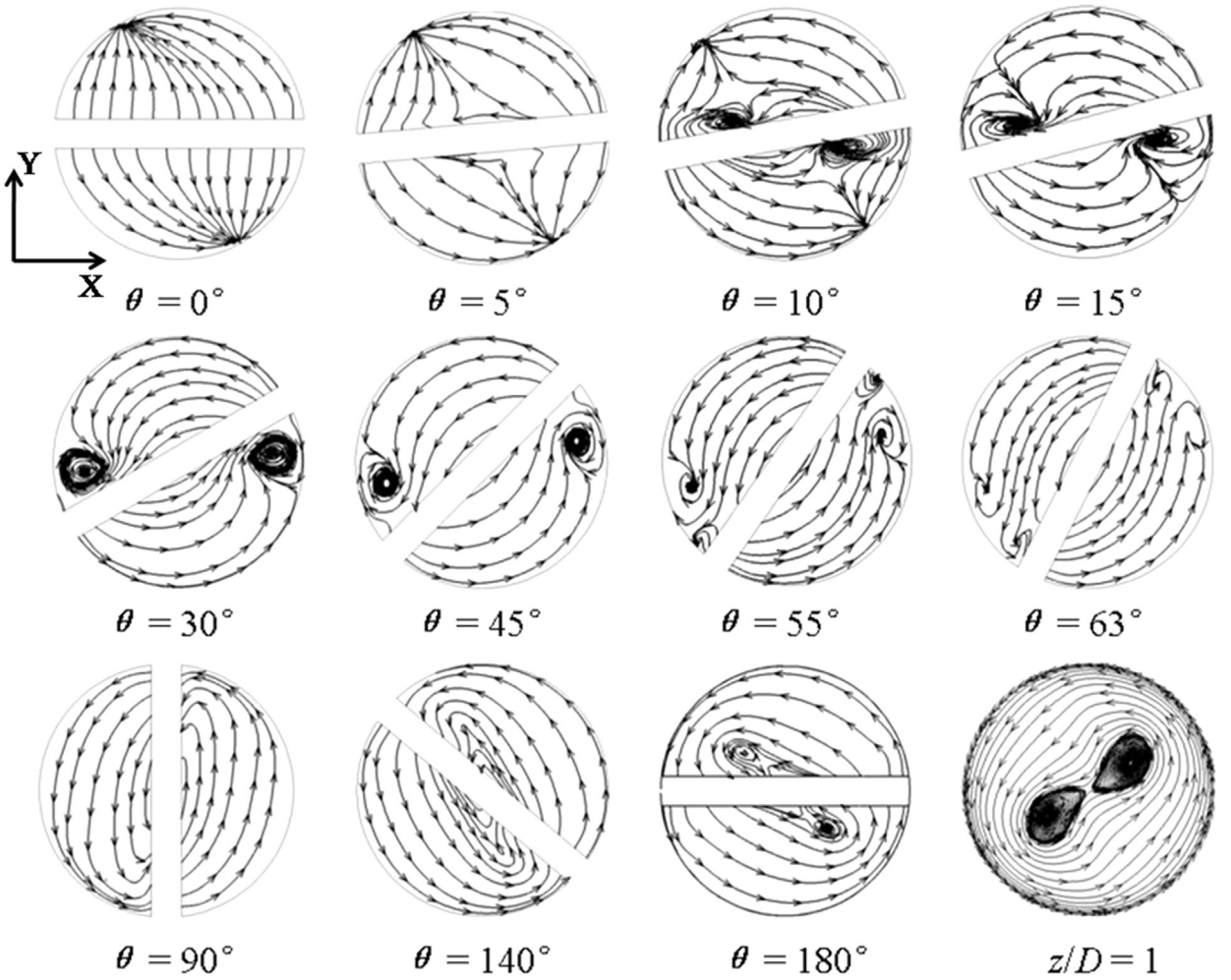

Fig. 5. Helical vortices formation process inside the twisted tape, tape twists counter clockwise, θ equals $(1+z/H)\times 180^\circ$ and represents axial positions. The positions of X and Y axes are the same for all 2D contour plots in this study.

3.2. Formation of helical vortices

The formation process of helical vortices is shown in Fig.5. As the fluid enters the twisted tape, the flow is split under the effect of leading edge of the twisted tape. In the region of the twisted tape, two vortices appear and strength near the inlet, rotating counter relative to the tape twist (θ=10–30°). Both two vortices decay under the influence of tangential velocity of the main flow (θ=30° and 45°). During these vortices decaying process, two corotating vortices appear, and these four vortices coexist temporarily (θ=55° and 63°). After those vortices disappear (θ=90° and 140°), two corotating helical vortices exist (θ=180 °). Downstream of the twisted tape, the corotating secondary vortices remain inside the straight pipe (z/D=1). It implies the formation process of helical vortices needs enough twisted degree.

The formation mechanism of corotating vortices is shown in Fig. 6. Considered the torsion effect of the twisted tape, the system can be considered as a semicircular channel rotates around the pipe center point, hence the presence of Coriolis force is assumed. As the fluid enters the twisted tape, the flow is split under the effect of leading edge of the twisted tape, shown in Fig. 6a and b. At 10° of twist, under the effect of Coriolis force, the pressure near the left corner is low, and adverse pressure gradient presents near the left corner. Streamlines bend seriously as the adverse pressure gradient here. Due to the conservation law of angular momentum, the vortex rotates counter to the twisted tape, shown in Fig. 6(c). The vortex develops and strengthens, seen θ=10°, 15° and 30° in Fig. 6. It is shown that Coriolis force, which is assumed as the presence of torsion, plays a dominant role near the twisted tape inlet. The force which causes high pressure gradient and curved streamlines, can promote the formation of vortices.

Another corotating vortex appears during the vortex decaying process, and the two vortices rotate counter coexist, seen in Fig. 6(d). In this region, the strength of counter rotation vortices gradually decreases. The low pressure region returns to the pipe center under the effect of centrifugal force. With the rotating tape, the vertical distance between counter rotating vortex and twisted tape surface becomes large, and enough room here is to form vortex. The wall shear stress reduces to

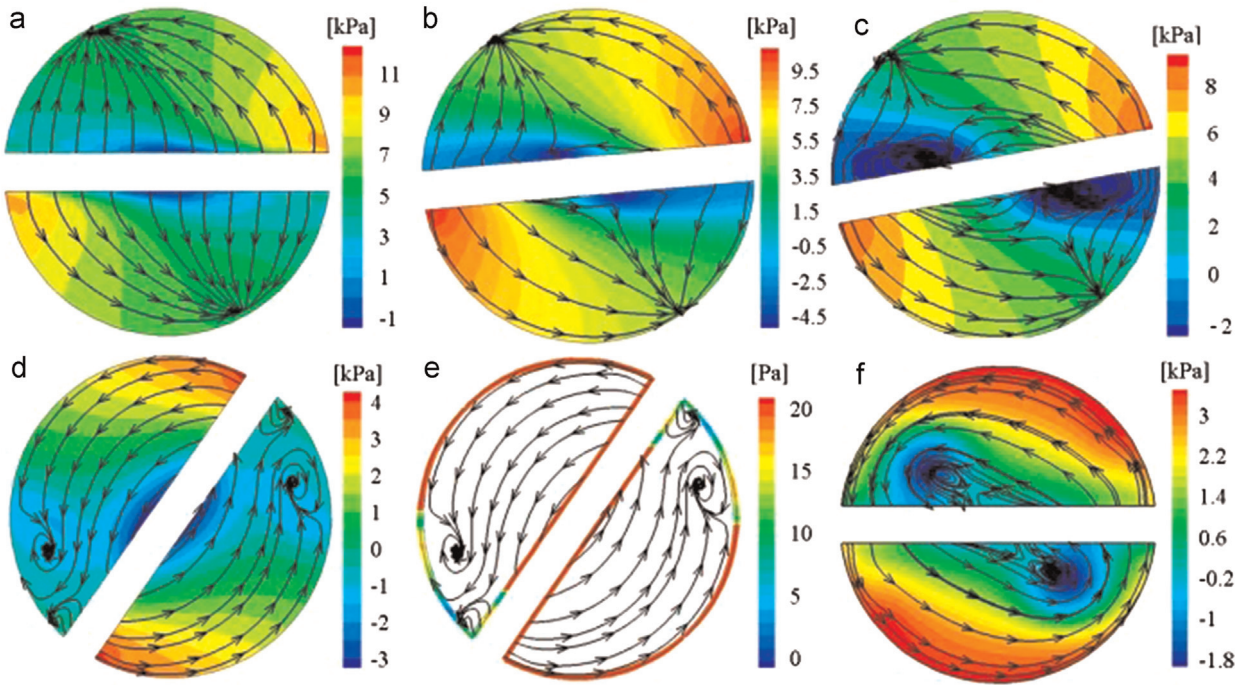

Fig. 6. Static pressure, streamlines and wall shear stress at different streamwise positions: (a) static pressure and streamlines at $\theta=0°$, (b) static pressure and streamlines at $\theta=5°$, (c) static pressure and streamlines at $\theta=10°$, (d) static pressure and streamlines at $\theta=55°$, (e) wall shear stress and streamlines at $\theta=55°$ and (f) static pressure and streamlines at $\theta=180°$.

zero shown in Fig. 6(e). Boundary layer separates, and a corotating vortex appears here. The pressure distribution at $\theta=180°$can be seen in Fig. 6(f), and helical vortices appear here. The low pressure region moves from pipe center to the top left (relative to the twisted tape) under the effect of Coriolis force. Streamlines bend to the low pressure core (seen $\theta=140°$ and 180° in Fig. 5) due to the pressure gradient. Corotating helical vortices form due to the flow unstability induced by streamlines deformation. Once the twisted tape ends, helical vortices remain downstream of the twisted tape. In general, as the development of flow, centrifugal force induced by the torsion of twisted tape causes the radial pressure gradient which promotes the formation of vortices. The position of low pressure region corresponding to the position of helical vortices is mainly influenced by Coriolis force.

3.3. Development of helical vortices

The intensity of secondary flow in swirling flow is characterized by J^n_{ABS}, the absolute vorticity flux. It is defined as follows [17]:

$$J^n_{ABS} = \frac{\iint_A |\omega_a| dA}{A} \tag{8}$$

The absolute vorticity flux denotes the averaged absolute vorticity flux of all vortices over the cross section, the parameter is used to reflect the intensity of helical vortices here.

The development of helical vortices can be seen in Fig. 7. The distribution of J^n_{ABS} along streamwise is shown in Fig. 7(a). During the development process of helical vorticies, the variation of vorticities distribution at different cross sections ($z/D=0.98$, 1.77, 5.9, 7.28 and 8.86) can be seen in Fig. 7(b). In the twisted tape region ($z/D<0$), the secondary flow is formed and strengthened, and the absolute vorticity flux increases with developing flow. Downstream of the twisted tape ($z/D>0$), vorticity distribution is dispersive under the effect of the twisted tape disturbing the flow, from 0.98 to 1.77 of z/D. As in the twisted tape region, fluid in each of the two semicircular channels develops alone. Once the fluid flows out of the twisted tape, the structures of helical vortices are not stable due to the sudden change of channel. The absolute vorticity flux decreases sharply. Away from the twisted tape, vortices are gradually stable ($z/D=1.77$–7.87). Away from the twisted tape ($z/D=7.87$–15.75), the flow structures of helical vortices are stable and vorticities are more concentrative.

The decay of helical vortices intensities along streamwise with variable Reynolds number ($Re=1.0\times10^5$, 8.9×10^4, 7.7×10^4, 5.1×10^4, 2.5×10^4) can be seen in Fig. 8. The intensity of helical vortices decays quickly near the twisted tape ($z/D=3.94$–7.87), and slowly away from the twisted tape($z/D=7.87$–15.75). The reason is that flow structures of vortices are not stable near the twisted tape outlet, shown in Fig. 7(b), and energy consumption is high here. Away from the tape, flow is

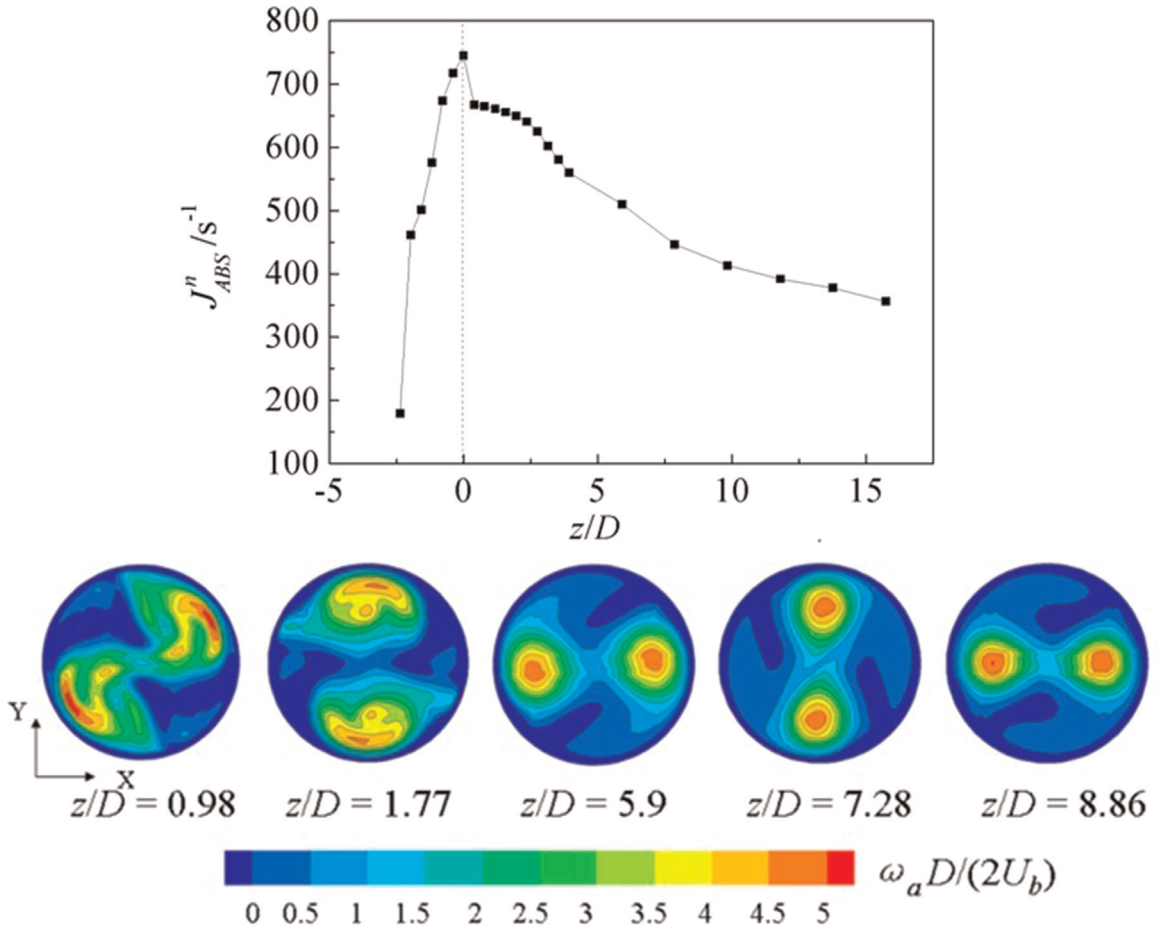

Fig. 7. Development of helical vortices. (a) variation of J^n_{ABS} along streamwise and (b) dimensionless vorticities of axial component distribution at different streamwise positions, U_b is the inlet velocity (3.03 m/s), D is the pipe diameter, and ω_a is the axial vorticity.

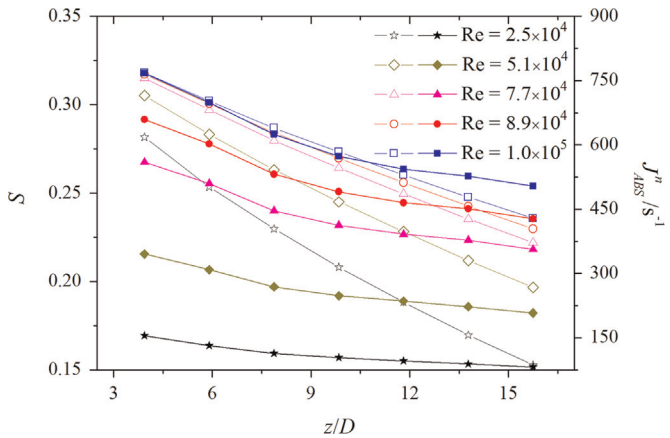

Fig. 8. Decay of absolute vorticity flux and swirl intensity for different Reynolds numbers along streamwise. The solid dot means absolute vorticity flux and hollow dot means swirl intensity.

fully developed, and the flow structures of vortices are gradually stable. The linear reducing absolute vorticity flux is mainly due to the vortex bending and viscous dissipation. The absolute vorticity flux increases with increasing Reynolds number, by comparing the curves of different Reynolds number. This trend is in agreement with the variation of swirl intensities. In this figure, the swirl intensities decay quickly compared with the helical vortices intensities.

4. Conclusions

Helical vortices in the turbulent swirling flow induced by the short twisted tape inside a circular pipe are studied numerically by using RSM to reveal their formation and development.

In terms of structures of vortices, two regions are divided: vortices formation in the twisted tape and development downstream of the twisted tape. Two symmetrical stable helical vortices are present downstream of the twisted tape and their intensities decrease during their development. In the swirling flow with the presence of helical vortices, tangential velocities increase sharply near the pipe wall, while decrease greatly in the vicinity of the pipe center. Two high and two low symmetrical radial velocity regions present, and the values of radial velocity cannot be neglected.

The vortices form in the twisted tape and remain the structure downstream of the twisted tape. Torsion promotes the formation of helical vortices. The intensities of helical vortices decay along the streamwise direction, and decay slowly than the intensities of swirling flow. With the increasing Reynolds numbers, the intensities of helical vortices increase.

Acknowledgment

The financial support from National Natural Science Foundation of China under the Contract no. 51276140 is appreciated.

References

[1] M.M. Abu-Khader, Further under-standing of twisted tape effects as tube insert for heat transfer enhancement, Heat Mass Transf. 43 (2006) 123–134.
[2] R.M. Manglik, A.E. Bergles, Heat transfer and pressure drop correlations for twisted-tape inserts in isothermal tubes (I) laminar flows, J. Heat Transf. Heat Transf. 115 (1993) 881–889.
[3] R.M. Manglik, A.E. Bergles, Heat transfer and pressure drop correlations for twisted-tape inserts in isothermal tubes (II) Transition and turbulent flows, J. Heat Transf. 115 (1993) 890–896.
[4] E.V. Seymour, Fluid flow through tubes containing twisted tapes, Engineer 111 (1966) 634–642.
[5] R.M. Manglik C. Ranganathan., Visualization of Swirl Flows Generated by Twisted-Tape Inserts in Circular Tubes, in: Proceedings of the 4th World Conference on Experimental Heat Transfer, Fluid Mechanics and Thermodynamics". Edzi oni ETS, Pisa, Italy 1997.
[6] L. You, Computational Modeling of Laminar Swirl Flows and Heat Transfer in Circular Tubes with Twisted-Tape Inserts, University of Cincinnati, Cincinnati, 2002.
[7] R.M. Manglik, Swirl flow heat transfer and pressure drop with twisted-tape inserts, Adv. Heat Transf. 36 (2004) 183–265.
[8] S. Eiamsa-ard, C. Thianpong, P. Eiamsa-ard, P. Promvonge, Convective heat transfer in a circular tube with short-length twisted tape insert, Int. Commun. Heat Mass Transf. 36 (2009) 365–371.
[9] O.H. Klepper, Heat transfer performance of short twisted tapes, AICHE J. 35 (1972) 1–24.
[10] C.K. Aidun, M. Parsheh, Spatially periodic reversing core in a twisted-fin generated swirling pipe flow, Phys. Fluids 19 (2007) 1–4.
[11] R. Cazan, C.K. Aidun, Experimental investigation of the swirling flow and the helical vortices induced by a twisted tape inside a circular pipe, Phy. Fluids 21 (2009) 1–9.
[12] A. Escue, J. Cui, Comparison of turbulence models in simulating swirling pipe flows, Appl. Math. Model. 34 (2010) 2840–2849.
[13] S. Eiamsa-ard, K. Wongcharee, S. Sripattanapipat, 3-D Numerical simulation of swirling flow and convective heat transfer in a circular tube induced by means of loose-fit twisted tapes, Int. Commun. Heat Mass Transf. 36 (2009) 947–955.
[14] F.S. Lien, M.A. Leschziner, Assessment of turbulent transport models including nonlinear RNG Eddy-viscosity formulation and second-moment closure, Comput. Fluids 23 (1994) 982–1004.
[15] S. Pope, Turbulent Flows, Cambridge Press, Cambridge, 2000.
[16] Fluent Inc., Fluent User's Guide., Fluent Inc., NH, Lebanon, 2003.
[17] Z.M. Lin, D.L. Sun, L.B. Wang, The relationship between absolute vorticity flux along the main flow and convection heat transfer in a tube inserting a twisted tape, Heat Mass Transf. 45 (2009) 1351–1363.
[18] A.K. Gupta, D.G. Lilley, N. Syred, Swirl Flow, Abacus Press, England, 1984.